Journal of Functional Materials and Applied Engineering

Research Paper

Effect of Montmorillonite Content on the Ordered Structure of Cellulose Nanofibrils-based Composite Film

Aragorn Legolas [1], Gimli Boromir [2], Michelle Nguyen [2,*]

1 School of Logistics, RMIT University College of Business, Melbourne, Australia
2 Department of Life Science , Swinburne University of Technology, Hawthorn, Australia
*Corresponding author: Aragornlegolas@rmit.edu.au; Boromir@swin.edu.au; Nguyen@gmail.com

Abstract. In this work, TEMPO-oxidized cellulose nanofibril (TOCNF)/montmorillonite (MMT) composite films were fabricated via the solution-casting method. The influences of MMT loading on the ordered-structure characteristics and structure-property relationships of TOCNF/MMT composite films were systematically investigated. The experimental results reveal that at an MMT content of 10 %-40 %, MMT nanosheets can stack regularly inside composite films to form dense ordered lamellar architectures. Such structures effectively facilitate interfacial stress transfer, which brings about a prominent improvement in the tensile strength of composite films, reaching a maximum value of 142.5 MPa (129 % of that of pure TOCNF film). Meanwhile, the composite films retain high optical transmittance (~92 %) and low haze (~5 %). Nevertheless, when the MMT content rises to 50 %-80 %, agglomerates with diameters of 1-3 μm emerge within the composite matrix. These agglomerates degrade the regularity of lamellar structures and trigger local structural disorder. Disordered domains induce stress concentration and lead to severe deterioration of mechanical properties, with tensile strength dropping as low as 44.9 MPa. Moreover, disordered structures increase the porosity and pore size of composite films, multiply the interfacial boundaries among TOCNF, MMT and air, and intensify light-scattering effects. Consequently, the optical transmittance decreases to 90.4 %-78.6 %, while the haze increases sharply to 37.7 %-52.9 %.

Keywords: c*ellulose nanofibrils; montmorillonite; ordered structure; structure-property relationship*

Received on 02 July 2024, Accepted on 05 Nov 2024, Published on 15 Dec 2024

1 Introduction

Vigorous development of biomass-derived materials constitutes one of the vital approaches to relieve resource shortages and mitigate “white pollution”[1-2]. Natural biomass materials generally exhibit multi-hierarchical structural features. Their ordered organization across different length-scales provides important references for constructing high-performance green materials[3-4]. For instance, nacre seashells possess a highly ordered “brick-and-mortar” architecture alternately stacked by inorganic aragonite platelets and organic matrices, which endows nacre with outstanding mechanical performance combining high strength, high toughness and high hardness[5-6]. The concept of bionic structural design has been widely adopted for fabricating high-performance composite materials.

Cellulose nanofibrils (CNF), originating from plant cell walls, are promising renewable nanomaterials featuring low density, high strength, favorable thermal stability and excellent film-forming capacity[7-8]. Montmorillonite (MMT) is an abundantly available layered silicate mineral in nature. It can be exfoliated into two-dimensional nanosheets upon ultrasonic treatment, possessing high modulus, large specific surface area and excellent ion-exchange capacity[9]. Both CNF and MMT can be stably dispersed in aqueous systems. They exhibit favorable matching in structural dimension and interfacial interactions, making them ideal building blocks for fabricating biomass-based composite films with bionic nacre-inspired “brick-and-mortar” structures. In recent years, CNF/MMT composite films have demonstrated great potential to substitute conventional petroleum-based plastics in fields including flexible electronic devices[10], high-barrier films[11-13] and nanofluidics[14].

Furthermore, nanocellulose films show promising prospects in oxygen- and water-vapor-barrier applications[15], and have gradually become an important research hotspot for biomass-based functional films[16-17].

Constructing well-ordered "brick-and-mortar" architectures is critical for preparing high-performance CNF/MMT composite films[18]. Multiple strategies can be adopted to optimize their ordered structures: ① Regulation of film-fabrication routes, such as layer-by-layer assembly[19], vacuum filtration[20], solution casting[16] and freeze-casting[21]. Among these techniques, solution casting relies on water-evaporation-induced self-assembly. It can effectively modulate the drying procedure and realize oriented platelet arrangement, and thus has gained wide application. ② Exfoliation of bulk MMT into single-layer nanosheets. Wu et al.[22] successfully obtained fully-exfoliated synthetic saponite nanosheets via high-pressure homogenization combined with sonication. They blended saponite with CNF and cast the mixture to fabricate high-strength transparent CNF/saponite composite films. ③ Improvement of dispersion stability for single-layer MMT. CNF can act as a green dispersant to stabilize single-layer MMT in aqueous media[23], facilitating ordered stacking during film formation. Ming Siyi et al.[24] prepared transparent flame-retardant composite films by dispersing single-layer clay with CNF, achieving a transmittance up to 90 %.

Nevertheless, obvious deterioration in optical and mechanical properties frequently occurs for CNF/MMT composite films with elevated MMT content. Wu et al.[25] fabricated CNF/MMT composite films with 5 % MMT loading via water-evaporation-induced self-assembly. The material delivered ultra-high tensile strength (509 MPa), high Young's modulus (18 GPa) and excellent toughness (\(25.6\ \mathrm{MJ/m^{3}}\)), while maintaining transmittance of approximately 80 %. CNF/MMT composite films can realize ultra-high tensile strength and good transparency at low MMT loadings. Once MMT content exceeds a certain threshold, the transmittance drops sharply and mechanical performance degrades correspondingly. This phenomenon indicates that MMT content governs the comprehensive performance of composite films by altering stacking modes and ordering degree of single-layer MMT during water-evaporation-driven self-assembly. However, systematic investigations are still lacking regarding the structural-evolution pathways of single-layer MMT under different MMT contents throughout self-assembly, as well as how such evolution influences mechanical and optical performances of composite films.

Accordingly, in this study, TEMPO-oxidized cellulose nanofibrils (TOCNF) were used as dispersing agent. Stable single-layer MMT dispersion was obtained by ultrasonic exfoliation combined with centrifugal classification. Solution-casting method was employed to prepare TOCNF/MMT composite films with varied MMT contents (10 %-80 %, with 10 % increment intervals). Emphasis was placed on characterizing the ordering degree of lamellar structures modulated by MMT loading. Correlations between ordered structures and mechanical performances (tensile strength, toughness, elastic modulus), as well as optical performances (transmittance, haze) were analyzed. This work aims to reveal the evolution rules of lamellar ordered structures in TOCNF/MMT composite films as a function of component ratio, and the corresponding structure-property relationships between microstructure and mechanical-optical behaviors. It is expected to provide references for structural design and performance tuning of high-strength transparent biomass-based composite films.

2 Experimental

2.1 Raw Materials and Reagents

Bleached softwood kraft pulp, supplied by Canfor Corporation (Canada); montmorillonite (MMT, purity ≥ 98 %, powder, average particle size 16-22 μm), purchased from Nanocor (USA); 2,2,6,6-tetramethylpiperidin-1-oxyl (TEMPO, mass fraction 98 %), Shanghai Macklin Biochemical Co., Ltd.; sodium hypochlorite (NaClO, solid, available chlorine ≥ 60 %), sodium bromide (NaBr, analytical grade), sodium hydroxide (NaOH, solid, analytical grade), Guangzhou Chemical Reagent Technology Co., Ltd.

2.2 Instruments and Equipment

LC-MP-31 dual-channel pH-conductivity meter, Lichen-Boxi Instrument Technology (Shanghai) Co., Ltd.; Mini-Type high-pressure microfluidizer, Noz Fluid Technology (Shanghai) Co., Ltd.; SCIENTZ-IID ultrasonic cell disruptor, Ningbo Scientz Biotechnology Co., Ltd.; DL-5000B refrigerated centrifuge, Shanghai Anting Scientific

Instrument Factory; PicoForce atomic force microscope (AFM), Bruker (USA); LHS-50CL constant-temperature-and-humidity chamber, Shanghai Yiheng Scientific Instrument Co., Ltd.; Instron 3300 universal material testing machine, Instron (USA); UV-2600i Plus UV-Vis spectrophotometer, Shimadzu (Japan); X'pert Powder multi-position automatic-sample-changing X-ray diffractometer (XRD), PANalytical (Netherlands); SU5000 field-emission scanning electron microscope (FESEM), Hitachi (Japan).

2.3 Experimental Procedures

2.3.1 Preparation of TOCNF

Bleached softwood kraft pulp was pretreated by alkaline TEMPO-oxidation system[26]. The reacted pulp slurry was further processed by high-pressure homogenization to obtain TEMPO-oxidized cellulose nanofibrils (TOCNF). Detailed procedures are described below. The available-chlorine content of NaClO reagent was calibrated according to GB/T 19106-2013.

5 g oven-dry bleached softwood kraft pulp was dispersed in 200 mL deionized water. 0.1 mmol TEMPO and 1 mmol NaBr were each dissolved in 100 mL deionized water. The three components were transferred together into a 1 L round-bottom flask and stirred to achieve homogeneous mixing. NaClO with required dosage (calculated as 8 mmol per gram of oven-dry pulp, based on available chlorine) was dissolved in 100 mL deionized water to prepare NaClO solution. NaClO solution was added drop-wise into the round-bottom flask. 1 mol/L NaOH solution was adopted to maintain the pH of reaction system at 10.0-10.5. The reaction proceeded at room temperature. Terminate the reaction when the color of reaction liquid changes from yellow to white and system pH keeps constant within 10 min. Afterwards, the pulp slurry was repeatedly filtered and washed with deionized water until the filtrate reached neutral pH. The TEMPO-pre-oxidized pulp was diluted to a pulp consistency of 0.5 %. High-pressure microfluidizer homogenization was performed: once at 34.5 MPa, twice at 69.0 MPa, and one additional pass at 138.0 MPa. Large incompletely disintegrated fibers were removed by filtration with a 1500-mesh filter bag (pore size 17 μm), and TOCNF suspension was finally obtained.

2.3.2 Preparation of Single-Layer MMT Dispersion

0.1 g oven-dry TOCNF suspension was uniformly dispersed in deionized water (total mass 99 g). Under stirring at 2000 r/min, 1 g MMT powder was slowly added to obtain crude TOCNF/MMT suspension. The crude suspension was treated by ultrasonic cell disruptor at 420 W for 20 min. The treated suspension was transferred into a refrigerated centrifuge and centrifuged at 5000 r/min for 30 min. The supernatant liquid was collected as TOCNF-stabilized single-layer MMT dispersion (hereinafter referred to as single-layer MMT dispersion).

2.3.3 Fabrication of TOCNF/MMT Composite Films

TOCNF/MMT composite films were prepared by solution-casting method. Polystyrene Petri dishes with 10 cm diameter were used as casting molds. Predetermined amounts of single-layer MMT dispersion and TOCNF dispersion were weighed and mixed in beakers under magnetic stirring. Deionized water was supplemented to dilute the mixed system to a mass fraction of approximately 0.25 %, followed by continuous stirring for thorough homogenization. The beaker was placed inside a vacuum-drying cabinet for vacuum degassing. The fully defoamed mixture was slowly poured into molds, and then dried in a constant-temperature-and-humidity chamber set at 40 °C and 65 % relative humidity to yield TOCNF/MMT composite films. The as-prepared films were conditioned for 24 h in a constant-temperature-and-humidity room (23 °C, 50 % relative humidity). Film mass was weighed with electronic analytical balance, and thickness was measured by electronic thickness gauge, so as to calculate the actual basis weight and compactness of composite films.

2.4 Characterization and Testing

2.4.1 Morphology Characterization of TOCNF and MMT Dispersions

AFM was utilized to characterize the morphology of TOCNF and MMT dispersions. Freshly cleaved fluoromica sheets were fixed onto iron substrates. Test dispersions were diluted to 5 mg/L and fully dispersed by ultrasonic cleaner. 25 μL dispersion was drop-cast onto mica sheets, which were subsequently dried by infrared heater. Dried mica samples were mounted on the AFM sample stage, and probes were installed for morphological observation.

2.4.2 Crystallinity Characterization of Composite Films

XRD powder diffraction measurement in continuous-scan mode was carried out. Cu Kα radiation was adopted, X-ray wavelength 0.154 nm, 2θ scanning range 4°-40°, step size 0.13°.

2.4.3 Mechanical-Property Testing of Composite Films

Composite films were cut into specimen strips of 5 cm × 1 cm. Thickness values were recorded at five separate positions for each strip. Tensile tests were performed on universal material testing machine equipped with a 20 kN load cell. Test parameters: tensile rate 1.25 mm/min, gauge length 1 cm. Ten parallel replicates were measured for each sample group to acquire tensile strength, elastic modulus and toughness. Elastic modulus was automatically calculated by Bluehill software from stress-strain curves.

2.4.4 Optical-Property Characterization

The UV-Vis spectrophotometer was used to test the optical transmittance and haze of composite films. A blank substrate was calibrated before measurement. Film specimens with dimensions of 4 cm × 4 cm were fixed inside the instrument sample cell. The scanning wavelength was set from 300 nm to 800 nm, and three parallel specimens were tested for each group of samples. The average value was recorded to obtain light-transmittance-wavelength curves and haze data.

2.4.5 Micro-Morphology Observation of Composite-Film Cross-Sections

Composite-film samples were cryo-fractured in liquid nitrogen to obtain flat cross-section surfaces. Specimens were fixed on conductive adhesive and subjected to gold-sputtering pretreatment. Afterwards, cross-section micro-morphologies of the composite films were observed via field-emission scanning electron microscopy under an accelerating voltage of 5 kV.

3 Results and Discussion

3.1 Morphology of TOCNF and Single-Layer MMT

Figure 1 presents AFM images and corresponding height profiles of TOCNF and single-layer MMT nanosheets. As shown in Figure 1(a) and 1(b), the prepared TOCNF exhibits typical nanofibril morphology with a fibril height of approximately 2.5 nm. The TOCNF fibrils are uniformly dispersed without obvious aggregation. Figure 1(c) and 1(d) show that the exfoliated MMT displays sheet-like nanostructures; the statistical sheet thickness is around 1.2 nm, which is consistent with the theoretical thickness of single-layer montmorillonite. The above results prove that single-layer MMT nanosheets and well-dispersed TOCNF were successfully prepared in this experiment.

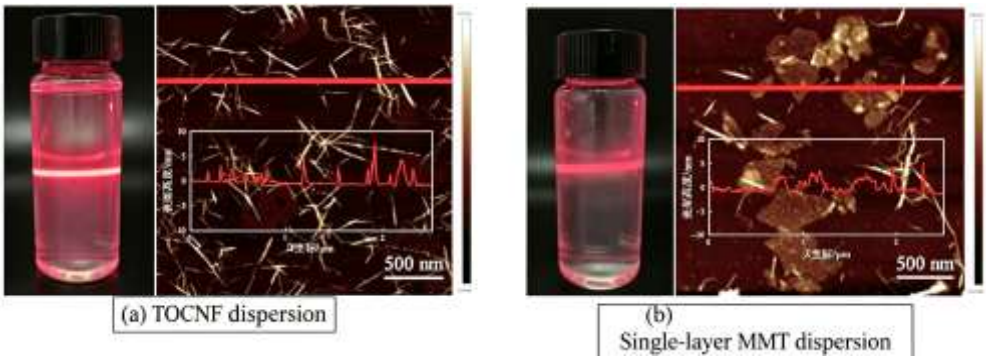

Figure 1 Appearance and AFM images of TOCNF and monolayer MMT

3.2 XRD Analysis of TOCNF/MMT Composite Films

Figure 2 displays XRD patterns of pure MMT powder, pure TOCNF film and TOCNF/MMT composite films with

different MMT mass fractions. Pure MMT powder shows a strong characteristic diffraction peak at 2theta=7.1o, corresponding to the (001) crystal plane of montmorillonite, and its basal spacing {001} equals 1.24 nm. The pure TOCNF film exhibits typical diffraction peaks of cellulose I at 2theta=14.8 o, 16.4 o and 22.6 o.

For TOCNF/MMT composite films with MMT content of 10 %-40 %, the (001) diffraction peak of MMT shifts toward lower angles, and the calculated basal spacing {001} increases to 1.38-1.46 nm. This phenomenon indicates that TOCNF molecules intercalate between MMT nanosheets, enlarging interlayer spacing and forming ordered lamellar stacking structures. When MMT mass fraction rises to 50 %-80 %, the (001) diffraction peak of MMT moves back toward high angles, and the basal spacing drops to 1.25-1.29 nm. This suggests that excessive MMT loading triggers restacking and re-aggregation of partial MMT nanosheets, which reduces interlayer spacing and destroys the highly ordered lamellar arrangement inside composite films.

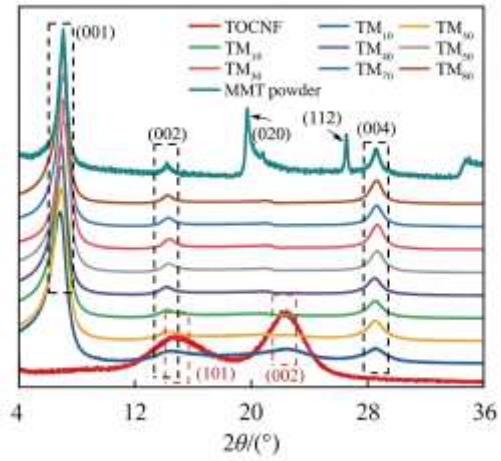

Figure 2 XRD patterns of TOCNF film, TOCNF/MMT composite films, and MMT powder

Table 1 Basic Experimental Parameters for Preparing TOCNF/MMT Composite Films

Sample ID	MMT Mass Fraction / %	TOCNF Mass Fraction / %	Total Solid Content of Casting Suspension / wt%	Drying Temperature / ℃	Relative Humidity / %
T-0	0	100	0.25	40	65
T-10	10	90	0.25	40	65
T-20	20	80	0.25	40	65
T-30	30	70	0.25	40	65
T-40	40	60	0.25	40	65
T-50	50	50	0.25	40	65
T-60	60	40	0.25	40	65
T-70	70	30	0.25	40	65
T-80	80	20	0.25	40	65

3.3 Cross-Sectional Micro-Morphology of TOCNF/MMT Composite Films

Figure 3 shows cross-section FE-SEM images of TOCNF/MMT composite films with different MMT contents. The pure TOCNF film (Figure 3a) possesses a relatively dense cross-section with disordered fiber stacking and no obvious layered texture. When MMT content is 10 %-40 % (Figure 3b-3d), numerous alternating “brick-and-mortar” lamellar structures can be clearly observed on cross-sections. MMT nanosheets are horizontally oriented and orderly stacked, and TOCNF fills gaps between MMT nanosheets, constructing highly ordered layered architectures. Such ordered lamellar structures are favorable for efficient interfacial stress transfer between TOCNF and MMT.

As MMT content further increases to 50 %-80 % (Figure 3e-3h), large-size MMT agglomeration zones with diameters of 1-3 μm emerge in the cross-sectional field of view. Inside these agglomeration regions, MMT nanosheets are randomly oriented, the regular lamellar texture disappears, and massive disordered structural domains are generated. The occurrence of disordered domains breaks the continuity of ordered lamellar structures, which is in good agreement with the XRD analysis results. Excessive MMT addition leads to severe agglomeration of nanosheets during solution-casting self-assembly, producing mixed microstructures coexisting with ordered lamellae and disordered agglomerates.

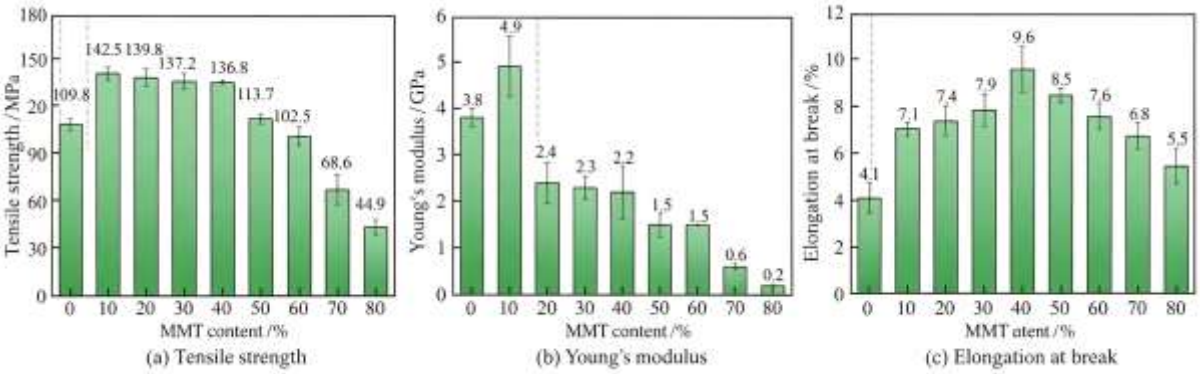

Figure 3 Mechanical properties of TOCNF film and TOCNF/MMT composite films

3.4 Mechanical Properties of TOCNF/MMT Composite Films

Figure 4 summarizes the mechanical-property test results of TOCNF/MMT composite films with different MMT contents, including tensile strength, elastic modulus and toughness. As shown in Figure 4(a), with the increase of MMT content from 0 % to 40 %, the tensile strength of composite films rises continuously. At 40 % MMT loading, the tensile strength reaches the maximum value of 142.5 MPa, which is 129 % of the tensile strength of pure TOCNF film (110.5 MPa). This improvement originates from the well-ordered “brick-and-mortar” lamellar structure formed inside the composite film. Oriented-stacked MMT nanosheets bear major external loads, and hydrogen-bond-rich TOCNF matrices serve as binding phases to realize effective interfacial stress transfer, thus significantly reinforcing tensile performance.

Nevertheless, once MMT content exceeds 40 %, tensile strength declines sharply. When MMT content reaches 80 %, tensile strength falls to merely 44.9 MPa. Combined with cross-section SEM observations, excessive MMT induces the formation of large-scale disordered agglomeration domains. Stress-concentration points are easily produced at agglomeration boundaries under external tension, which initiate microcracks and accelerate crack propagation, finally resulting in prominent deterioration of tensile strength.

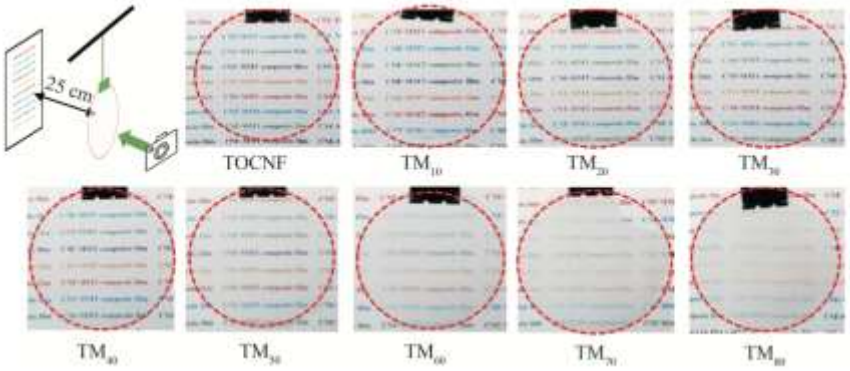

Figure 4 Photo of TOCNF film and TOCNF/MMT composite films

The variation trend of elastic modulus is similar to that of tensile strength (Figure 4b). The elastic modulus increases gradually within the MMT content range of 0-40 % and achieves the maximum value of 10.8 GPa at 40 % MMT. After MMT content surpasses 40 %, elastic modulus decreases markedly. As illustrated in Figure 4(c), the toughness of composite films keeps decreasing monotonously with the growth of MMT content. Even within the ordered-structure region of 10-40 % MMT, the introduction of rigid MMT nanosheets restricts the sliding and deformation of TOCNF molecular chains, resulting in reduced toughness of composite films. After entering the high-MMT-content disordered-domain region, crack-propagation pathways are shortened by agglomerated defects, which further lowers the toughness of composite materials.

3.5 Optical Properties of TOCNF/MMT Composite Films

Figure 5 displays optical transmittance (550 nm wavelength) and haze data of TOCNF/MMT composite films with varied MMT contents. In the MMT-content interval of 0-40 %, composite films maintain high optical transmittance of approximately 92 %, and the haze remains at a low level of about 5 %. Under such conditions, MMT nanosheets are uniformly and orderly stacked, and few internal defects exist inside the film matrix. The size of MMT nanosheets is far smaller than visible-light wavelength, so light scattering is weak and excellent optical transparency is retained.

When MMT content increases from 50 % to 80 %, optical transmittance drops from 90.4 % down to 78.6 %, while haze rises steeply from 37.7 % to 52.9 %. Massive MMT agglomerates with micrometer-scale sizes are generated in the disordered-structure zone. These agglomerates and abundant internal interfaces among TOCNF, MMT and air pores strongly scatter incident visible light, which brings about decreased transmittance and sharply elevated haze. The above results demonstrate that MMT content exerts decisive influences on optical performances by regulating the internal microstructure of composite films.

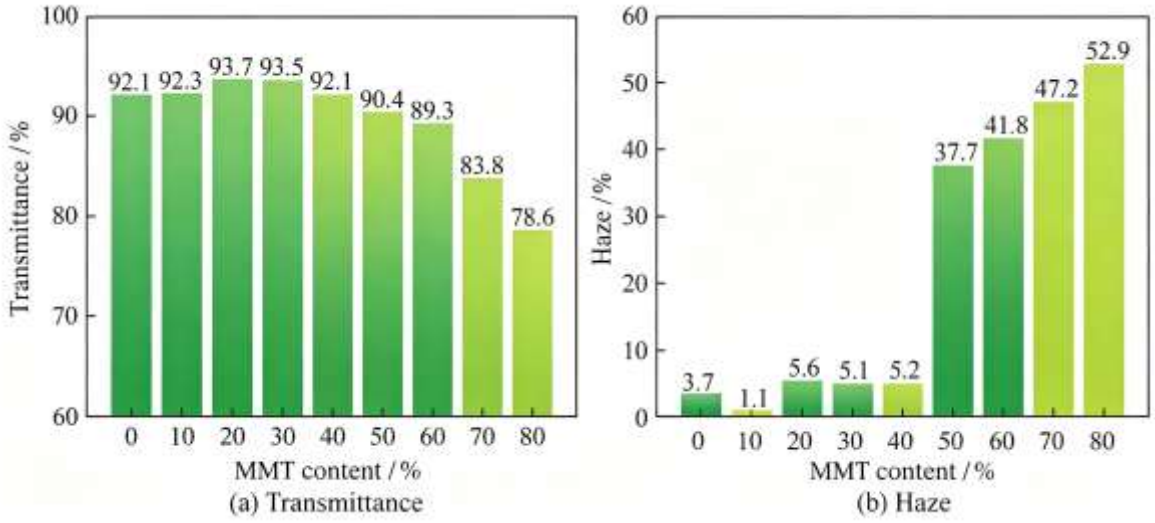

Figure 5 Optical properties of TOCNF film and TOCNF/MMT composite films

3.6 Evolution of Layered-Ordered Structure in TOCNF/MMT Composite Films Regulated by MMT Content

Figures 6 and 7 show field-emission scanning electron microscope (FESEM) images of tensile fracture surfaces of pure TOCNF film and TOCNF/MMT composite films with different MMT contents, so as to characterize the influence of MMT content on the structural ordering of composite-film lamellae. As shown in Figure 6, the fracture surface of pure TOCNF film is relatively dense and continuous. Although it exhibits a certain tendency of lamellar orientation, local undulations and wrinkles can be observed with poorly-ordered arrangement. When the MMT content ranges from 10 % to 40 %, progressively better-defined and more regularly-arranged lamellar structures form on the fracture surfaces of composite films. This indicates that the introduction of MMT nanosheets together with their co-orientation with TOCNF during evaporation-induced self-assembly plays a vital role in constructing layered-ordered architectures. Specifically, for composite films with 10 %-40 % MMT loading,

fracture surfaces display continuous and densely stacked lamellar features.

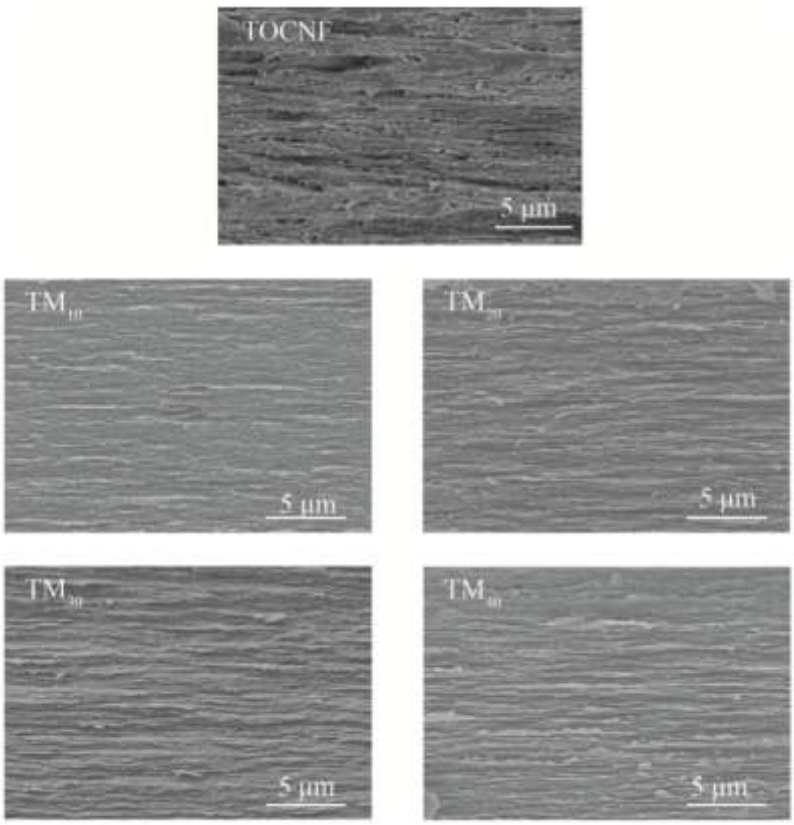

Figure 6 Cross-sectional FESEM images of TOCNF film and TOCNF/MMT composite films (MMT contents ≤40%)

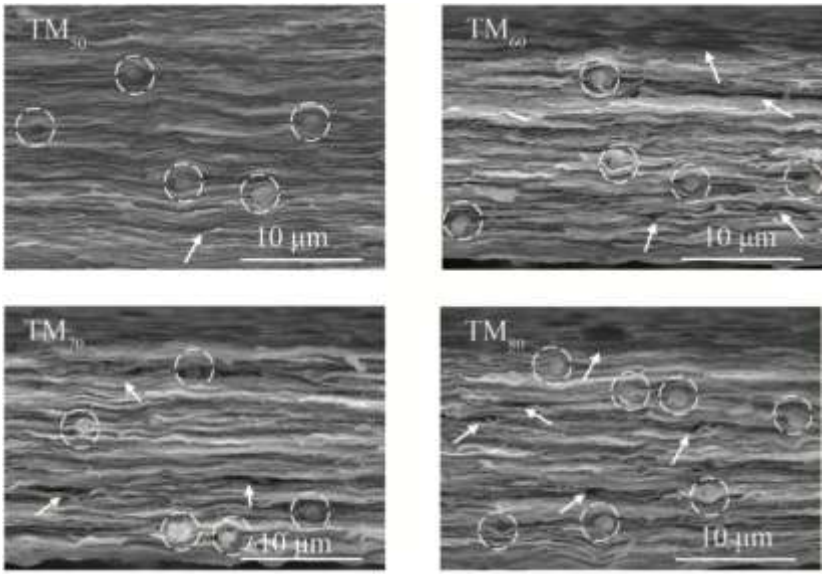

Figure 7 Cross-sectional FESEM images of TOCNF/MMT composite films (MMT contents≥50%)

Monolayer MMT nanosheets align roughly parallel to the film plane, with no obvious pores or large-sized defects detected. This finding demonstrates that at relatively low MMT contents, MMT maintains good dispersion within

the TOCNF matrix. During water evaporation, MMT nanosheets gradually orient and stack in monolayer form, which facilitates the construction of dense ordered lamellar structures and inhibits further flocculation into large-scale agglomerates.

When MMT content rises to 50 %-80 %, micrometer-sized agglomerates with diameters of 1-3 μm appear inside composite films. Inside these agglomerated regions, MMT nanosheets are randomly oriented; the regular lamellar texture disappears and abundant disordered structural domains are generated. The occurrence of disordered domains disrupts the continuity of ordered lamellar structures, which matches the XRD test results well. Excess MMT loading triggers severe nanosheet agglomeration in the course of solution-casting self-assembly, producing mixed microstructures where ordered lamellae and disordered agglomerated domains co-exist.

3.7 Correlation Between Ordered-Structure Evolution and Comprehensive Performance of Composite Films

Combined with the above-mentioned test results of mechanical and optical properties, the structure-performance evolution mechanism of TOCNF/MMT composite films can be summarized as follows (Figure 8).

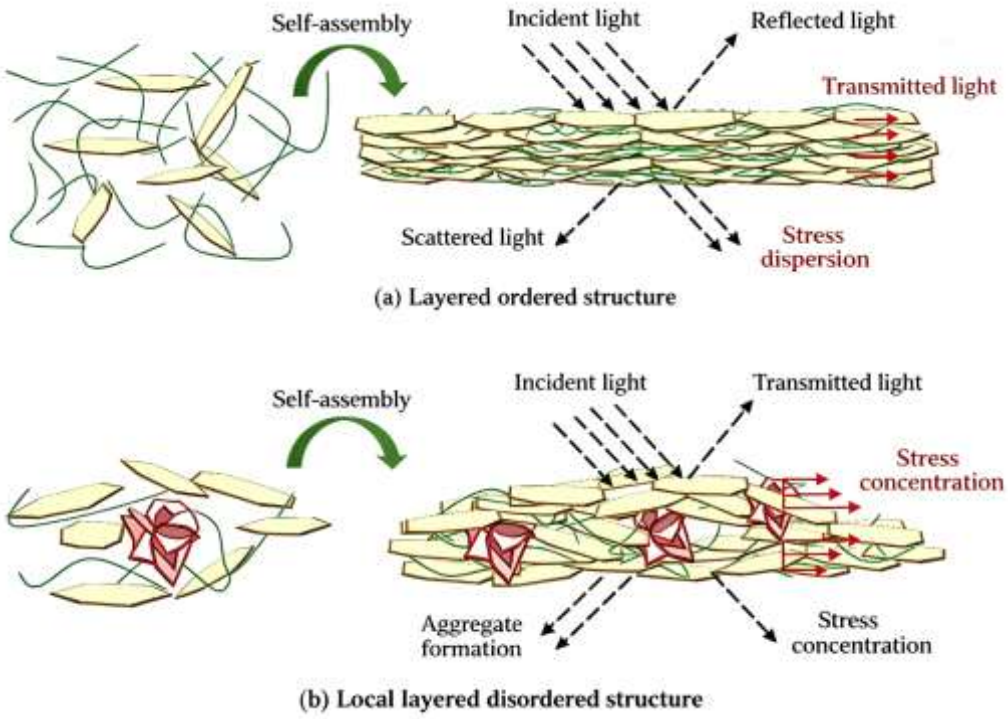

Figure 8 Schematic illustration of the relationship between the evolution of layered ordered structure and the mechanical and optical properties of TOCNF/MMT composite film

Within the MMT-content range of 10 %-40 %: MMT nanosheets are homogeneously dispersed in the TOCNF aqueous suspension. Driven by capillary forces during water-evaporation-induced self-assembly of solution casting, MMT nanosheets achieve horizontal orientation and regular stacking. TOCNF molecular chains intercalate between MMT layers and fill gaps among nanosheets, building highly ordered bionic “brick-and-mortar” lamellar architectures. Such ordered lamellar structures greatly improve the efficiency of interfacial stress transfer. Therefore, tensile strength and elastic modulus of composite films are significantly enhanced. Meanwhile, no large-size agglomeration defects form inside the matrix. Since the size of MMT nanosheets is far smaller than the wavelength of visible light, light-scattering effect is weak. Consequently, composite films retain high visible-light transmittance and low haze.

Within the MMT-content range of 50 %-80 %: excessive MMT nanosheets tend to restack and agglomerate in

aqueous systems. During solvent evaporation, micrometer-scale disordered agglomerated domains emerge inside composite films, destroying the continuity of ordered lamellar structures. These disordered agglomerates act as internal structural defects. From the mechanical perspective, stress-concentration zones easily generate at defect boundaries under external loading, inducing microcrack initiation and accelerating crack propagation, which leads to sharp deterioration of tensile strength and elastic modulus. From the optical perspective, micrometer-sized agglomerates as well as newly-formed pore-interface defects intensify visible-light scattering, resulting in reduced transmittance and a dramatic rise in haze.

This work investigates solution-cast composite films built from TEMPO-oxidized cellulose nanofibrils (TOCNF) and exfoliated montmorillonite (MMT) nanosheets, focusing on how MMT loading dictates lamellar ordering and further modulates mechanical and optical performances. The core performance variations originate from microstructure evolution driven by water-evaporation-induced self-assembly, including well-ordered nacre-like “brick-and-mortar” stacking at moderate filler fractions and destructive nanosheet agglomeration under excessive MMT addition.

Properly exfoliated single-layer MMT nanosheets are essential prerequisites for constructing high-performance films. Ultrasonic exfoliation and centrifugal classification produce MMT sheets around 1.2 nm thick, which can be stably dispersed in aqueous TOCNF suspension owing to interfacial compatibility between negatively charged TOCNF fibrils and MMT surfaces. During solution casting, water evaporation generates capillary force that guides component rearrangement. Within the optimal MMT content window of 10 %-40 %, MMT nanosheets maintain homogeneous dispersion and gradually orient parallel to the film plane. TOCNF chains intercalate between clay layers, expanding MMT basal spacing and filling interstitial spaces between inorganic platelets, which jointly assemble continuous, dense, ordered lamellar “brick-and-mortar” architectures analogous to natural nacre, as validated by XRD and cross-sectional FESEM observations.

Such well-organized layered microstructures are responsible for prominent mechanical reinforcement. Rigid, high-modulus MMT nanosheets serve as load-bearing “bricks”, while hydrogen-bond-rich TOCNF matrices act as flexible organic “mortar”. Abundant interfacial hydrogen-bonding interactions between TOCNF and MMT enable efficient interfacial stress transfer across alternating organic-inorganic layers under external tensile loading. Stress can be widely distributed throughout the ordered lamellar network rather than concentrating at local sites. Consequently, tensile strength reaches the maximum value of 142.5 MPa at 40 wt% MMT, equivalent to 129 % of pure TOCNF film strength, accompanied by improved elastic modulus. Nevertheless, the rigid inorganic platelets restrict the sliding and plastic deformation of cellulose molecular chains, leading to a gradual decline in film toughness even within this favourable composition range. In terms of optical properties, uniformly oriented monolayer MMT possesses lateral dimensions far smaller than visible-light wavelengths. Few micrometre-sized defects or voids exist inside the compact matrix, so light-scattering effects are largely suppressed. Therefore, composite films retain high optical transmittance near 92 % and low haze around 5 %.

Once MMT mass fraction rises above the 40 % threshold (50 %-80 %), the self-assembly behaviour changes drastically. Excessive MMT nanosheets cannot be fully stabilized by limited TOCNF molecules in the aqueous system, and spontaneous restacking and aggregation occur prior to and during solvent evaporation. Large micrometre-scale agglomerates (1-3 μm in diameter) emerge inside the solidified film matrix, breaking the continuity of regular lamellar stacking and generating widespread disordered domains. XRD results confirm the shrinkage of MMT basal spacing, indicating the collapse of intercalated ordered structures. Mechanically, these agglomerated clusters act as intrinsic structural defects. Under tensile force, stress concentrates sharply around defect boundaries, readily triggering microcrack nucleation and accelerating crack propagation pathways across the composite. This accounts for the severe deterioration of tensile strength, which drops to as low as 44.9 MPa at 80 % MMT loading. Optically, micrometre-sized MMT agglomerates, together with newly-formed pores and multiply increased heterogeneous interfaces among TOCNF, MMT and trapped air, produce intense visible-light scattering. As a result, optical transmittance decreases progressively from 90.4 % to 78.6 %, while haze surges from 37.7 % up to 52.9 %.

Overall, MMT content functions as a critical switch governing self-assembly pathways and final microstructure. Moderate addition facilitates the formation of bioinspired ordered lamellar structures to realize balanced high strength and good transparency; over-dosing causes detrimental agglomeration and disorder, degrading both

mechanical and optical performances. This structure-property mechanism provides clear guidance for designing high-performance, transparent biomass-derived composite films.

4 Conclusions

In this work, TEMPO-oxidized cellulose nanofibril (TOCNF)/montmorillonite (MMT) composite films with different MMT contents were prepared via solution-casting self-assembly. The influences of MMT content on the evolution of lamellar-ordered structures and the structure-property relationships of composite films were systematically investigated. The main conclusions are drawn as follows:

(1) When MMT content is 10 %-40 %, MMT nanosheets realize regular horizontal stacking within the TOCNF matrix and form typical bionic “brick-and-mortar” ordered lamellar architectures. Ordered structures optimize interfacial-stress-transfer efficiency. At an MMT content of 40 %, the composite film reaches a maximum tensile strength of 142.5 MPa (129 % of that of pure TOCNF film), while maintaining high transmittance (~92 %) and low haze (~5 %).

(2) When MMT content increases to 50 %-80 %, a large number of micrometer-scale MMT agglomerated domains form inside composite films. MMT nanosheets are randomly oriented, ordered lamellar structures are destroyed. Disordered structural domains produce stress-concentration defects, and the tensile strength drops as low as 44.9 MPa. At the same time, intensified light-scattering effect decreases transmittance to 78.6 %-90.4 % and increases haze to 37.7 %-52.9 %.

(3) MMT content governs the evolution of microstructural ordering degree of TOCNF/MMT composite films. Appropriate MMT addition facilitates the formation of ordered “brick-and-mortar” lamellar structures and realizes synergistic improvement of mechanical and optical performances. Excess MMT triggers nanosheet agglomeration and generates disordered defective domains, causing simultaneous degradation of both mechanical and optical properties. This study provides experimental support for microstructural design and performance optimization of high-strength transparent cellulose-nanofibril-based composite films.

References

[1] LI T, ZHANG X, WANG Y, et al. Strong, tough, and biodegradable cellulose-based structural materials[J]. Advanced Materials, 2022, 34(21): e2108954.
[2] WANG S, LU A, ZHANG L. Recent advances in regenerated cellulose materials[J]. Progress in Polymer Science, 2016, 53: 169-207.
[3] MEYERS M A, CHEN P Y, LIN A Y M, et al. Biological materials: Structure and mechanical properties[J]. Progress in Materials Science, 2008, 53(1): 1-206.
[4] WEGST U G K, BAI H, SAIZ E, et al. Bioinspired structural materials[J]. Nature Materials, 2015, 14(1): 23-36.
[5] SUN J, BHUSHAN B. Hierarchical structure and mechanical properties of nacre: A review[J]. RSC Advances, 2012, 2(20): 7617-7632.
[6] BARTOLO R, BURGHARDT W R, KISAILUS D. Nacre-inspired polymer-clay nanocomposites: A review[J]. Progress in Materials Science, 2021, 121:101838.
[7] HABIBI Y, LUCIA L A, ROJAS O J. Cellulose nanocrystals: Chemistry, self-assembly, and applications[J]. Chemical Reviews, 2010, 110(6): 3479-3500.
[8] NECHYPORCHUK O, SMIRNOV I, LARSSON P A, et al. Cellulose nanofibrils-based materials for technical applications[J]. Advanced Materials, 2021, 33(28): e2001064.
[9] BERGAOUI L, MAKHLOUFI A, BOUHADDI A, et al. Montmorillonite clay: A review of its structure and applications[J]. Applied Clay Science, 2022, 223:106525.
[10] ZHANG Y, ZHANG L, LI B, et al. Flexible transparent conductive films based on cellulose nanofibrils[J]. Carbohydrate Polymers, 2023, 312:116817.
[11] WU C, YANG Q, ZHANG K, et al. Ultrastrong cellulose-montmorillonite composite films with high oxygen-barrier performance[J]. Advanced Functional Materials, 2020, 30(13):1909359.
[12] LIU Y, LIU J, WANG H, et al. High-barrier cellulose-clay composite films: A review[J]. Progress in Organic Coatings, 2024, 188:107936.

[13] SONG M, GONG J, LIU Y, et al. Multifunctional cellulose-nanofibril-montmorillonite composite coatings for food-packaging applications[J]. Food Chemistry, 2024, 470:131394.
[14] MA R, WANG J, YANG X, et al. Nanofluidic membranes constructed by cellulose-nanofibril-montmorillonite layered nanostructures[J]. ACS Nano, 2023, 17(8): 7845-7855.
[15] NOBILE M A. Barrier properties of nanocellulose-based films and coatings: A review[J]. Trends in Food Science & Technology, 2022, 124: 148-161.
[16] WU Q, MENG S, ZHENG Y, et al. Self-assembled cellulose-nanofibril-clay composite films with nacre-like structure[J]. Composites Science and Technology, 2022, 221:109341.
[17] MENG S, WU Q, FANG Z Q. Recent progress on nacre-mimetic cellulose-nanofibril-clay composite materials[J]. Chinese Journal of Polymer Science, 2024, 42(5): 721-738.
[18] ZHENG Y, WU Q, FANG Z Q. Design strategies of ordered nacre-inspired cellulose-based composite films[J]. Materials Chemistry Frontiers, 2023, 7(18): 4077-4096.
[19] ZHANG L, LI Y, WANG X, et al. Layer-by-layer assembled cellulose-montmorillonite multilayer films[J]. Cellulose, 2021, 28(11): 7241-7254.
[20] HUANG J, ZHU H, ZHANG Y, et al. Vacuum-filtered nacre-like cellulose-clay composite films[J]. Composites Part A: Applied Science and Manufacturing, 2020, 137:106012.
[21] XU T, ZHANG K, SONG P, et al. Freeze-cast anisotropic cellulose-montmorillonite porous composites[J]. Carbohydrate Polymers, 2022, 288:119415.
[22] WU Q, MENG S, FANG Z Q. High-strength transparent composite films of cellulose nanofibrils and synthetic saponite nanosheets[J]. Composites Communications, 2023, 39:101586.
[23] MENG S, WU Q, FANG Z Q. Cellulose nanofibrils as green dispersants for exfoliating and stabilizing montmorillonite nanosheets[J]. Journal of Colloid and Interface Science, 2023, 642: 410-419.
[24] MENG S Y, WU Q, FANG Z Q. Transparent flame-retardant composite films based on cellulose-nanofibril-stabilized clay nanosheets[J]. Cellulose, 2024, 31(7): 4347-4360.
[25] WU Q, MENG S, ZHENG Y, et al. Ultra-strong transparent cellulose-montmorillonite nacre-mimetic composite films with high toughness[J]. Advanced Science, 2022, 9(22): e2202817.
[26] SAITO T, KIMURA S, NISHIYAMA Y, et al. Cellulose nanofibers prepared by TEMPO-mediated oxidation of native cellulose[J]. Biomacromolecules, 2007, 8(8): 2485-2491.